This article has been accepted for publication in a future issue of this journal, but has not been fully edited. Content may change prior to final publication. Citation information: DOI 10.1109/TPWRS.2018.2812711, IEEE Transactions on Power Systems

A Hybrid Bat Algorithm for Economic Dispatch with Random Wind Power

Huijun Liang, Yungang Liu, Yanjun Shen, Fengzhong Li, Yongchao Man

***Abstract*—We present a hybrid metaheuristic optimization algorithm for solving economic dispatch problems in power systems. The proposed algorithm, based on bat algorithm, combines chaotic map and random black hole model together. Chaotic map is used to prevent premature convergence, and the random black hole model is helpful not only in avoiding premature convergence, but also in increasing the global search ability, enlarging exploitation area and accelerating convergence speed. The pseudo code and related parameters of the proposed algorithm are also given in the paper. Different from other related works, the costs of conventional thermal generators and random wind power are both included in the cost function because of the increasing penetration of wind power. The proposed algorithm has no requirement on the convexity or continuous differentiability of the cost function, although the effect on fuel cost, caused by the underestimation and overestimation of wind power, is included. This makes it feasible to take more practical nonlinear constraints into account, such as prohibited operating zones and ramp rate limits. Three test cases are given to illustrate the effectiveness of the proposed method.**

***Index Terms*—economic dispatch, power systems, bat algorithm, random black hole, chaotic map.**

I. Introduction

ECONOMIC dispatch problem (EDP) is one of the central concerns in power systems, whose objective is to economize operating costs for all committed generators while meeting the supply-demand balance and constraints such as active power generation limits, ramp rate limits and prohibited operation zones [1], [2]. As a constrained optimization problem, EDP can be solved by λ-iteration method [3], gradient method [4] and projection method [5]. But these conventional mathematical methods require cost functions to be continuously differentiable and convex, and hence can not be applied to EDP since the presence of ramp rate limits, prohibited operation zones and valve-point effects makes the involved cost functions inevitably discontinuous and/or nonconvex.

In the past two decades, intelligent metaheuristic algorithms have been applied to EDP, without requiring the cost function to be continuous or convex (see e.g., [6]–[14] and references therein). Specifically, in [6] and [7], GA and improved GA were employed to solve EDP with valve-point effects. In [8]–[11], PSO and hybrid PSO algorithms were employed for solving EDP with nonlinear features, which are caused by prohibited operation zones, ramp rate limits and valve-point effects. In [12], artificial bee colony optimization algorithm was presented for multi-area economic dispatch. In [13], a modified harmony search algorithm was proposed for EDP considering the effect of environment. In [14], a hybrid harmony search algorithm was developed for solving EDP, as well as the multi-area EDP. However, all the aforementioned works are only concerned with thermal generators and do not involve renewable energies.

Recently, a variety of renewable energy have been integrated in power systems to cope with the challenge of environment and the shortage of energy. Among them, *wind power* (which means the active power generated by wind turbines in this paper) are a typical, widely used manner. It was reported that the installed capacity of wind turbines reached 456 GW around the world in 2016 [15]. Therefore, it is urgent to integrate random wind power into EDP. In this direction, there has been much progress. In [16], virtual power plant technology was used for EDP incorporating wind turbines, but the wind farms were assumed to be zero cost, which means no penalty for the underestimation and overestimation of available wind power. In [17], thermal generators were included in the cost function, but wind turbines were treated as a constraint. GA was employed to solve EDP with wind turbines in [18], but the cost function only includes thermal generators and the cost caused by random wind power is ignored. A distributed economic dispatch method with random wind power was realized in [19], but requires the existence of gradient of the cost function, which is not always satisfied due to the nonlinear characteristics caused by valve-point effect, prohibited operation zones, etc.

Bat algorithm, which is proposed in 2010 and inspired by the echo locative behavior of bats, is much superior to GA and PSO in terms of accuracy and efficiency [20]. The effectiveness of bat algorithm for solving engineering optimization problems was demonstrated in [21]–[24]. Specially, chaotic

Manuscript received May 20, 2017; revised January 21, 2018 and accepted March 1, 2018. This work was supported in part by the National Natural Science Foundation of China under Grant 61325016, Grant 61374028, Grant 61603217 and Grant 61703237, by the Natural Science Foundation of Shandong Province under Grant ZR2016FB07 and Grant ZR2017BF034, and by the China Post-Doctoral Science Foundation Funded Project under Grant 2016M602142 and Grant 2017M610424. (Corresponding author: Yungang Liu.)

H. J. Liang, Y. G. Liu, F. Z. Li and Y. C. Man are with the School of Control Science and Engineering, Shandong University, Jinan, 250061, China (e-mail: eric_liang@mail.sdu.edu.cn; lygfr@sdu.edu.cn; lifz@mail.sdu.edu.cn; ycman@mail.sdu.edu.cn).

Y. J. Shen is with the College of Electrical Engineering & New Energy, China Three Gorges University, Yichang, 443002, China (e-mail: shenyj@ctgu.edu.cn).

This article has been accepted for publication in a future issue of this journal, but has not been fully edited. Content may change prior to final publication. Citation information: DOI 10.1109/TPWRS.2018.2812711, IEEE Transactions on Power Systems

map was combined with bat algorithm in [22] which concluded that sinusoidal map was the most suitable chaotic map to replace loudness or pulse emission rate in bat algorithm. In [23], three approaches were pointed out to enhance the performance of bat algorithm, and the authors got the idea that bat algorithm hybridization with other algorithm was the most effective way to enhance its performance. Up to now, there have been only a few works on EDP via bat algorithm. For example, the chaotic bat algorithm [22] was applied to EDP in [27], but only thermal generators were considered in the model.

In this paper, we are concerned with the EDP incorporating thermal generators and wind turbines, and a novel hybrid bat algorithm (named **RCBA**) is proposed to deal with this problem by integrating **Random black hole model** and **Chaotic maps** into **bat algorithm**. The cases without wind turbines are also discussed for comparison with other algorithms to illustrate the effectiveness of the proposed algorithm. Specifically, the main contributions of this paper are two-fold:

$(\boldsymbol{i})$ *A new hybrid bat algorithm (RCBA) is provided which has good characteristics in performance enhancing compared with bat algorithm.* On one hand, the loudness and/or pulse emission rate are replaced by chaotic maps due to its good random characteristic. This is helpful in improving the diversity of solutions, and hence can reduce premature convergence problem. On the other hand, the random black hole model is integrated in RCBA to replace the local random walk in bat algorithm. This can greatly help increase the global search ability and enlarge exploitation area at current group best, and is key to acquire better solution and faster convergence speed for RCBA.

$(\boldsymbol{ii})$ *An effective method for solving EDPs including thermal generators and wind turbines is realized by the usage of RCBA.* The cost function in this paper contains not only the cost of conventional thermal generators but also the effect on fuel cost caused by the underestimation and overestimation of random wind power, unlike in [3]–[13] without involving random wind power. Due to the usage of RCBA, the convexity or continuous differentiability, as in [17] and [19], is not required for the cost function and constraints. So the proposed method can better match the reality in power systems. Particularly, the nonlinear constraints, such as ramp rate limits and prohibited operating zones, can be included in the model while considering the underestimation and overestimation of wind power.

The remainder of this paper is organized as follows. Section II elaborates the model of EDP including thermal generators and wind turbines. In Section III, RCBA is proposed and the process of implementing RCBA to EDP is presented. In Section IV, the superiority of RCBA is addressed with five typical benchmark functions, and three test cases are given to illustrate the effectiveness of RCBA. Remarks and future research directions are included in Section V.

II. Problem Formulation

The objective of EDP in this paper is to minimize the total costs including thermal generators and wind turbines subject to the constraints such as generator constraints and supply-demand balance.

A. Objective function

The cost function of EDP incorporating wind turbines is given by

$$\sum_{i=1}^{N_g} f_i(P_i) + \sum_{j=1}^{N_w} g_j(W_j), \tag{1}$$

where P_i and W_j are active power produced by the *i*-th thermal generator and the *j*-th wind turbine, respectively; N_g and N_w are the numbers of thermal generators and wind turbines, respectively. The cost function of the *i*-th thermal generator is described as:

$$f_i(P_i) \quad = \quad \alpha_i P_i^2 + b_i P_i + c_i, \tag{2}$$

where a_i, b_i, c_i are cost coefficients of the *i*-th thermal generator. The cost function of the *j*-th wind turbine is given by [29], [30]:

$$g_j(W_j) = q_j W_j + C_{rw,j} E(Y_{oe,j}) + C_{pw,j} E(Y_{ue,j}), \tag{3}$$

where q_j is the cost coefficient; $C_{rw,j}$ represents the cost coefficient for there exists remainder energies of the j-th available wind power (which is underestimation), and $C_{pw,j}$ represents the cost coefficient for purchasing electric power from other manners so as to make up the shortage of wind power (which is overestimation); $C_{rw,j}(E(Y_{oe,j}))$ and $C_{pw,j}(E(Y_{ue,j}))$ denote the costs of overestimation and underestimation for the j-th wind turbine, respectively. Interested readers are referred to [30] for the definitions of $E(Y_{oe,j})$ and $E(Y_{ue,j})$ due to the space limitation. In (1), the costs including thermal generators and wind turbines are integrated into the same cost function, and both underestimation and overestimation of the available wind power are considered due to the random nature of wind. We adopt this random wind power model in the cost function because it is especially suitable for analysis in EDP.

B. Constraint conditions

Constraints of the active power output limit for the *i*-th thermal generator, the *j*-th wind turbine and supply-demand balance are given by

$$P_i^{\min} \le P_i \le P_i^{\max}, \tag{4}$$

$$W_j^{\min} \le W_j \le W_j^{\max}, \tag{5}$$

$$\textstyle\sum_{i=1}^{N_g} P_i + \sum_{j=1}^{N_w} W_j = P_d + P_{\text{loss}}, \tag{6}$$

where $P_i^{\min}$ and $P_i^{\max}$ denote the minimum and maximum active power output of the i-th thermal generator, respectively; $W_j^{\min}$ and $W_j^{\max}$ denote the minimum and maximum active power output of the j-th available wind power, respectively;

P_d is the total load demand, and P_{loss} is the transmission line losses represented by B-coefficients, which is described as below:

$$P_{\text{loss}} = \sum_{i=1}^{N_g}\sum_{j=1}^{N_g} P_i B_{ij} P_j + \sum_{i=1}^{N_g} B_{0i} P_i + B_{00}. \tag{7}$$

Additionally, two practical operation constraints of thermal generators should be included in EDP.

(i) *Ramp rate limits* The ramp characteristics in starting up and shutting down generators are modeled as follows:

$$\begin{cases} P_i - P_i^0 & \leq UR_i, \\ P_i^0 - P_i & \leq DR_i, \end{cases} \tag{8}$$

where P_i^0, UR_i and DR_i denote the previous active power output, the limit of up-ramp rate, and the limit of down-ramp rate of the i-th thermal generator, respectively.

(ii) *Prohibited operating zones* A typical thermal unit may have a steam valve in operation or a vibration in a shaft bearing, which may cause discontinuity input-output performance curve. This phenomenon is called prohibited operating zones, which is described as below:

$$\begin{cases} P_i^{\min} \leq P_i \leq P_{i,1}^l, \\ P_{i,k-1}^u \leq P_i \leq P_{i,k}^l, \\ P_{i,n_i}^u \leq P_i \leq P_i^{\max}, \\ k = 2, \ldots, n_i, \end{cases} \tag{9}$$

where n_i is the number of prohibited operation zones for the i-th unit, $P_{i,k}^l$ and $P_{i,k}^u$ are lower and upper bound of the k-th prohibited operation zone for the i-th unit, respectively.

III. Development of The Proposed Algorithm

This section is devoted to proposing the hybrid bat algorithm (RCBA) by integrating chaotic maps and random hole model, and moreover, presenting the pseudo code of the proposed algorithm.

A. Overview of bat algorithm

Bats use echolocation to detect preys or shelter obstacles. The typical range of frequencies of acoustic pulses emitted by bats is between 25kHz and 150kHz, and the pulses can last for a few milliseconds. The pulse emission rate, which can be accelerated to about 200 pulses per second, will increase dramatically when bats are close to the prey. More specifically, the pulse emission rate is inversely proportional to the distance of the prey, and meanwhile, the loudness of emitted pulses will be decreased when bats fly to the prey.

Bat algorithm mimics the behavior of bat hunting for prey. For each virtual bat, the pulse frequency f_i, velocity v_i^t and position x_i^t at time step *t* are defined by

$$f_i = f_{\min} + (f_{\max} - f_{\min})\beta, \tag{10}$$

$$v_i^{t+1} = v_i^t + (x_i^t - x_*^t) f_i, \tag{11}$$

$$x_i^{t+1} = x_i^t + v_i^{t+1}, \tag{12}$$

where $f_{\min}$ and $f_{\max}$ are the minimum and maximum frequency of emitted pulses, respectively; $\beta \in [0, 1]$ is a uniformly distributed random number; x_*^t is the current best position (or solution) at time step *t* in the current population.

A new search is then executed by local random walk:

$$x_{i,\text{new}}^{t+1} = x_*^t + \xi A^t, \tag{13}$$

where $\xi \in [-1, 1]$ is a random number, and A^t is the average loudness at time step t.

When bats succeed in finding their preys, the loudness A_i is decreased and the pulse emission rate r_i is increased. The two characteristics are described as follows:

$$A_i^{t+1} = \alpha A_i^t, \tag{14}$$

$$r_i^{t+1} = r_i^0 (1 - \exp(-\theta t)), \tag{15}$$

where $0 < \alpha < 1$ and $\theta > 0$ are constants, and $A_i^t \to 0$, $r_i^t \to r_i^0$ as $t \to \infty$. The pseudo code of bat algorithm is available in [20].

B. Chaotic maps

Recently, chaotic maps have been successfully applied in many optimization cases (by replacing the random parameters or variables in algorithms) [9], [22], [27], [38], [39]. Thanks to the nonrepetition characteristic of chaos, algorithms based on chaotic maps achieve more overall search abilities than the original algorithms [38]. Moreover, the characteristic is key for algorithms to escape from local optima and hence to avoid premature convergence [39].

In bat algorithm (see [20]), the local random walk is executed only when the random value is larger than the pulse emission rate r_i, but r_i increases as iteration goes on (see (15)), and hence the probability for executing the local random walk decreases. Similarly, noting from (14) that A_i decreases as iteration goes on, the probability for accepting the new solution also decreases. An effective approach for bat algorithm to avoid premature convergence is to substitute chaotic maps for r_i and A_i.

C. Random black hole model

Any mass, whose radius is smaller than its Schwarzschild radius, can become a black hole which has strong gravitational effects [25], [26]. The gravity is so strong that nothing can escape from inside it. In Schwarzschild radius, the escape speed is equal to the speed of light. Because no object goes faster than light, anything which passes through or crosses the boundary of a black hole will be absorbed including light.

Inspired by the concept of black hole, the RBH-PSO [28] is proposed. Every particle in RBH-PSO is regarded as a star in space, and its fitness value is gravity. Each particle is affected by the gravity of global optimum and local optimum at each iteration. The real solution is still unknown during this process. The solution, which at this stage is the present group best, is regarded as the base point of a black hole.

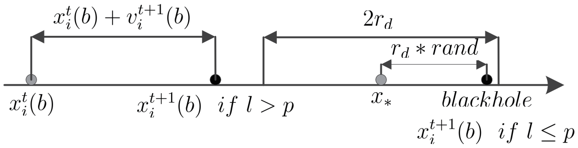

Fig. 1. Position update of $x_i^t(b)$ with random black hole.

We also adopt this random black hole model. The principle is described in Fig. 1 where $x_i^t(b)$ and $x_i^{t+1}(b)$ denote the b-th dimension's position of the i-th particle at time step t and $t+1$, respectively; $x_*^t(b)$ denotes the b-th dimension's position of current global optimum x_*^t (i.e., the base point) at time step t; r_d denotes the effective radius of a black hole; the threshold p and random value l represent the attraction of a black hole to stars and the coefficient corresponding to $x_i^t(b)$, respectively, which both obey uniform distribution in $[0,1]$.

A random black hole is generated close to the current group best x_*^t, and its distance to $x_*^t \in [-r_d, +r_d]$. Meanwhile, the threshold p associated to the black hole is also generated. Then for each single dimension $x_i^t(b)$ in every solution x_i^t, a random value l is generated, and $x_i^t(b)$ is captured by the black hole if $l \le p$, otherwise x_i^t will be updated by (12). The update rules are stated as follows:

$$x_i^{t+1}(b) = x_*^t(b) + r_d * \mu,\ l \le p, \tag{16}$$
$$x_i^{t+1} = x_i^t + v_i^{t+1},\ l > p, \tag{17}$$

where μ obeys uniform distribution in $[-1,1]$. The value for each dimension in x_i^t is updated individually by (16). But in bat algorithm, the values of all dimensions in x_i^t are updated simultaneously (see (13)).

The following aspects of benefits can be brought by integrating the random black hole model into bat algorithm:

(i) *Increase the global search ability.* Different from the actual black hole, the velocity v_i of all particles is kept and calculated at every iteration. Through this scheme, each dimension in a particle has the probability to be absorbed by the black hole and also has the chance to escape from the black hole in the next iteration. Therefore, the global search ability is enhanced greatly.

(ii) *Enlarge exploitation area and accelerate convergence speed.* Because the random black hole is generated around the current group best x_*^t, it is key to achieve a more accurate solution. On one hand, if x_*^t is near to the real global optimum, the model will give a complete search around x_*^t, which is helpful in accelerating convergence speed. On the other hand, if x_*^t gets into a local optimum, the model will help the particle to escape from the local minimum, which is helpful in avoiding premature convergence.

(iii) *Enhance the random search efficiency.* The effective radius r_d is treated as a piecewise parameter. At the beginning of iterations, for enlarging the search vision of individuals, r_d should be assigned with a relatively big value because the random initialized solutions are generally far away from the real global optimum. But as iteration goes on, a relatively good current group best is obtained, and an overlarge search vision would be harmful for individuals to find better solutions. So the value of r_d should be decreased to an appropriate interval. Particularly, r_d is independent of any other parameters and flexible to be used. This characteristic is meaningful in enhancing the random search efficiency.

Algorithm 1 Proposed algorithm: RCBA

Initialize bats population x_i, v_i, A_i^0,$f_{\min}$,$f_{\max}$ and r_i^0
Get fitness values according to the initial parameters
while $t <$ Max number of iterations **do**
  Generate p, μ and new solutions by (10), (11) and (12)
  if $rand > r_i^t$ **then** % Use black hole model here
    for each dimension in x_i^t **do**
      Randomly generate l
      Update $x_i^{t+1}(b)$ according to (16)
    end for
  end if
  Generate new fitness value f_{new} with x_i^{t+1}
  if $rand < A_i^t$ && $f_{\text{new}} < fitness(i)$ **then**
    Accept the new solution
  end if
  Rank the bats and find the current best x_*
  Update A_i^{t+1} and/or r_i^{t+1} by chaotic maps
end while
Post process results and visualization

D. Proposed algorithm

By integrating chaotic maps and random black hole model, we propose a new hybrid bat algorithm, named RCBA which is shown in Algorithm 1. Compared with bat algorithm, the proposed algorithm has the following superiorities:

(i) *The premature convergence problem is reduced.* As well known, evolutionary algorithms always encounter premature convergence problem. For example, PSO does when particles trap in some local optima [38]. As stated before, in our algorithm, chaotic map is meaningful for particles to escape from local optima, and the random black hole model can enlarge exploitation area. These help in avoiding premature convergence problem.

In this paper, A_i and/or r_i are updated by chaotic maps. For case 1 in Section IV, r_i is updated by sinusoidal map which is given as:

$$r_i^{t+1} = \zeta (r_i^t)^2 \sin(\pi r_i^t), \tag{18}$$

where ζ is set to 2.3. For cases 2 and 3 in Section IV, A_i and r_i are updated by

$$A_i^{t+1} = \begin{cases} A_i^t/0.7 & if\ A_i^t < 0.7, \\ 10(1-A_i^t)/3, & if\ A_i^t \ge 0.7, \end{cases} \tag{19}$$

and

$$r_i^{t+1} = r_i^t + 0.2 - ((0.5/(2\pi))\sin(2\pi * r_i^t)) \bmod 1, \tag{20}$$

This article has been accepted for publication in a future issue of this journal, but has not been fully edited. Content may change prior to final publication. Citation information: DOI 10.1109/TPWRS.2018.2812711, IEEE Transactions on Power Systems

respectively.

(ii) *The exploitation area is enlarged and the convergence speed is accelerated.* Bat algorithm uses local random walk to update positions. However, in RCBA, the local random walk is replaced by the random black hole model, which is helpful in increasing the global search ability, enlarging the exploitation area and accelerating convergence speed.

In RCBA, each dimension $x_i^t(b)$ in x_i^t is updated individually, and every iteration step has different updating parameters. This characteristic is illustrated by (16), where the base point x_*^t is updated at each end of iteration, and μ is a different random value in each iteration (see step 4 in Algorithm 1). The updating parameters are different because μ is changed and $x_*^t(b)$ may be modified at every iteration. So the exploitation area is increased greatly. But in bat algorithm, the update of x_i^t happens simultaneously for all dimensions, rather than only for one dimension; and meanwhile, the values for all dimensions in x_i^t are updated with the same parameter ξ at all iterations (see (13)). Therefore, the convergence speed in RCBA is more quickly than that in bat algorithm.

Actually, not all the dimensions in x_i^t will be updated in RCBA. The threshold p and random number l are changed at every iteration (see step 4 and 7 in Algorithm 1), and the value of every dimension $x_i^t(b)$ in x_i^t is updated only when $l \leq p$.

For the random black hole model, it is crucial to get the appropriate values of the radius r_d and the threshold p. If r_d is too large, the next solution will be far away from the global optimal solution. If r_d is too small, the function for enlarging visions will be lost. As for threshold p, it determines who has the chance to be absorbed by the black hole. An overlarge p will result in excessive dimensions in x_i^t to be updated, which is likely to have negative effect on convergence. When the threshold p is too small, the number of dimensions, whose values are updated in x_i^t, is very small, which would make the black hole model play a very limited effect on enhancing the ability for enlarging search areas and, hence, lead to a slower convergence speed than an appropriate value of threshold p.

E. Implement RCBA to EDP

The penalty function method is used to deal with the equality constraint (6), so the cost function (1) need to have a slight modification by using a penalty coefficient λ. Thus, we combine (1) with (6) and get the following objective function:

$$\begin{aligned}\sum_{i=1}^{N_g} f_i(P_i) \quad &+ \quad \sum_{j=1}^{N_w} g_j(W_j) \\ &+ \quad \lambda\left|\sum_{i=1}^{N_g} P_i + \sum_{j=1}^{N_w} W_j - P_d - P_{\text{loss}}\right|. \quad (21)\end{aligned}$$

By combining (4) and (8) we conclude

$$\max(P_i^{\min}, P_i^0 - DR_i) \leq P_i \leq \min(P_i^{\max}, P_i^0 + UR_i). \quad (22)$$

Then inequality constraints refer to (5), (9) and (22). The costs of $f_i(P_i)$ and $g_j(W_j)$ are defined by (2) and (3), respectively.

The steps for implementing EDP with RCBA are listed as follows:

Step 1: Obtain the parameters of thermal generators and wind turbines, and then generate the initial parameters for RCBA and the random black hole model.

Step 2: Generate the random initial solutions and get their fitness values using (21), and then find the best solution and the best fitness value.

Step 3: Update frequency f_i, velocity v_i^t and position x_i^t according to (10), (11), and (12), respectively.

Step 4: Generate the solution x_i^{t+1} by (16) or (17), and then check the inequality constraints (5), (9) and (22).

Step 5: Evaluate the new solution, update the loudness A_i^{t+1} and pulse emission rate r_i^{t+1}, and find the current best solution and the best fitness value.

Step 6: Repeat steps 3 to 5 until the stopping criterion is satisfied.

IV. EXAMPLES AND RESULTS

The superiority of RCBA is illustrated by five typical benchmark functions. Then, the effectiveness of the proposed method for power systems is demonstrated through three test systems: first, a 6-bus power system is used for solving EDP including thermal generators and wind turbines; second, a 26-bus system with 6 thermal generators and 46 transmission lines are contained in the simulation; third, a system with 38 generators is employed to illustrate the effectiveness of high dimensional system for power systems using RCBA. The unit of active power, fuel cost and CPU time are MW, \$/h, and second, respectively.

A. Simulation results with benchmark functions

This subsection illustrates the superiority of RCBA over other optimization algorithms with five typical benchmark functions, that is, Sphere, Ackley, Griewangk, Rastrigin and Rosenbrock. Readers can get the definitions of these functions in [31]. To better compare the performance of algorithms, four different dimensions (i.e., 2, 10, 30, 50) are considered for each benchmark function. The comparison results are shown in Tables I–IV.

TABLE I
RESULTS OF BENCHMARK FUNCTIONS WITH DIMENSION 2

Functions	RCBA	GA [33]	ICS [33]
Sphere	**2.0327E-47**	4.5E-9	1.2E-13
Ackley	**8.8818E-16**	6.3E-6	5.02E-7
Griewangk	**0**	–	–
Rastrigin	**0**	1.5E-8	6.5E-9
Rosenbrock	**4.4251E-23**	8.87E-5	5.10E-7

ICS: improved cuckoo search

Let's see what performance RCBA can have. In Table I, the dimension is set to 2, and RCBA obtains the smallest values among the three algorithms for all the listed benchmark

TABLE II
RESULTS OF BENCHMARK FUNCTIONS WITH DIMENSION 10

Functions	RCBA	CLPSO [31]	ABC [31]
Sphere	**3.8240E-44**	5.15E-29	4.86E-17
Ackley	8.8818E-16	4.32E-10	**2.3E-16**
Griewangk	**0**	4.56E-3	1.04E-3
Rastrigin	**0**	2.46	4.44E-17
Rosenbrock	**7.8494E-24**	8.87E-5	1.07E-1

CLPSO: comprehensive learning PSO; ABC: artificial bee colony

functions. In Table II, when the dimension is increased to 10, RCBA gets the optimum values for all the functions except Ackley. Table III shows the comparison results when the dimension is changed to 30, and the same phenomenon occurs as in Table I that RCBA gets the smallest values for all the functions. When the dimension is set to 50, as it shown in Table IV, RCBA outperforms other algorithms on the listed functions except Rastrigin. In short, RCBA nearly gets all the optimum values for the five benchmark functions under the four dimensions, which means that RCBA achieves better performance than the listed algorithms.

TABLE III
RESULTS OF BENCHMARK FUNCTIONS WITH DIMENSION 30

Functions	RCBA	GWO [34]	PSO [34]
Sphere	**3.0493E-43**	6.5900E-28	1.3600E-4
Ackley	**4.4409E-15**	1.0600E-13	2.7601E-1
Griewangk	**0**	4.4850E-3	9.2150E-3
Rastrigin	**2.5725E-3**	3.1052E-1	4.6704E1
Rosenbrock	**7.9403E-12**	2.6812E1	9.6718E1

GWO: grey wolf optimizer

TABLE IV
RESULTS OF BENCHMARK FUNCTIONS WITH DIMENSION 50

Functions	RCBA	ABC [31]	PSO [32]	FEA-PSO [32]	FEA-GA [32]
Sphere	**2.1E-42**	6.4E-16	3.60E-3	5.7E-17	9.39E-3
Ackley	**8E-15**	8.22	4.3E-14	1.3E-14	2.08E-2
Griewangk	**0**	4.4E-12	1.01E-2	9.10E-2	9.88E-2
Rastrigin	4.35E-4	**3.8E-13**	–	–	–
Rosenbrock	**7.32E-8**	3.08E1	6.09E1	2.99E0	7.38E1

FEA-PSO/GA: factored evolutionary algorithm-PSO/GA

The effective radius of random black hole is the key for RCBA to achieve such good performance and the Sphere function with dimension 30 is chosen to further elaborate this phenomenon. Fig. 2 shows the simulation results for Sphere function with five examples (each example has different value of r_d). To fairly compare the performance, the same random initialized values are used in the five examples. We first compare examples 3 and 4 (i.e., the dashed green line and the solid black line) which is shown in Fig. 2 (a). Both the two examples obtain relatively poor fitness values compared with other examples. The reason is that, the random initialized solutions are far away from the global optimum and the values of r_d for the two examples (i.e., $1e$-6 and $1e$-9, respectively) are too small. So the exploitation area is limited in a very small space. This is harmful for individuals to enlarge visions and accelerate convergence speed at the beginning. If this status is still continued, of course, a bad result would be obtained finally.

Fig. 2 (b) shows the remained three examples with a zoomed-in view as it is hardly to see them clearly in Fig. 2 (a). In Fig. 2 (b), the r_d's values of examples 1 and 2 are both relatively bigger than the corresponding values of examples 3 and 4 shown in Fig. 2 (a), and hence examples 1 and 2 get better convergence characteristics than examples 3 and 4. For themselves of examples 1 and 2, the convergence performance obtained by example 2 is superior to the performance obtained by example 1. This means that the effective radius of random black hole (i.e., r_d) can not be increased too much, which will affect the convergence performance adversely. But the value ($r_d = 1$) is also very important because the dashed red line (i.e., example 1) indicates that 1 is nearly the upper limit of r_d for Sphere function.

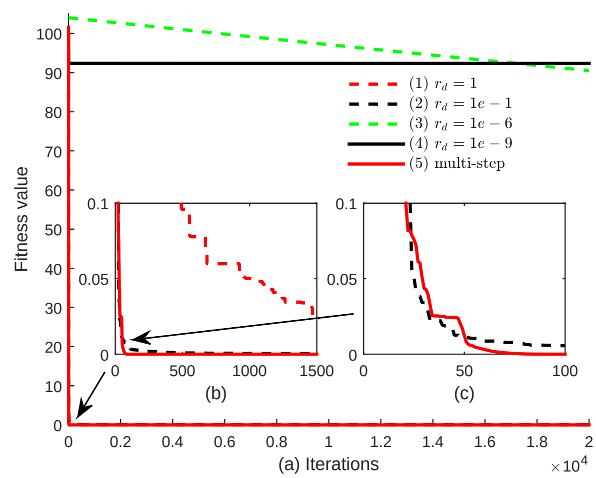

Fig. 2. (a) Simulation results for Sphere function with five examples. (b) A zoomed-in view for (a). (c) A zoomed-in view for (b).

TABLE V
THE PIECEWISE VALUES OF r_d AT DIFFERENT STEPS

Steps	[0, 50)	[50, 100)	[100, 200)	[200, 300)	[300, 400)
r_d	1e-1	1e-3	1e-4	1e-6	1e-9
Steps	[400, 500)	[500, 600)	[600, 700)	[700, 2e4)	
r_d	1e-12	1e-14	1e-17	1e-20	

All the above analysis stimulates us to propose a new idea, that is, can we treat r_d as a piecewise manner to enhance the performance of RCBA whenever at the beginning or at any other time of the iterations? Example 5 gives the answer. Fig. 2 (c), which is a zoomed-in view for Fig. 2 (b), shows the convergence curves of examples 2 and 5. The value of r_d for example 2 is 1e-1, but for example 5, r_d is characterized in a piecewise manner which is shown in Table V. Both the two examples have the same value of r_d at the steps of 1 to 50, and use the same random initialized values, so two relatively close solutions are obtained around the 50th step. But after this, example 5 achieves better convergence speed and optimum value than example 2 due to the decreased value of r_d as the iteration goes on. Therefore, the piecewise manner for r_d provides an effective approach for RCBA to achieve better performance.

To sum up, a better performance is achieved by RCBA compared with the listed algorithms, and the effective radius r_d plays a central role in RCBA.

B. Simulation results for EDP of power systems using RCBA

Three test cases are chosen to demonstrate the effectiveness of the proposed method. For the three test systems, in case 1 and 2, $p = 0.45$, and r_d is set to 42 and 2 when the steps in $[1, 25]$ and $[26, 500]$, respectively; and for case 3, r_d and p are set to 2 and 0.25, respectively. The parameters should be modified appropriately according to different occasions. Moreover, for convenience, thermal generator and wind turbine are simply denoted by TG and WT in the later figures and tables.

1) Case 1: *Implementation on a 6-bus system including random wind power*

In this case, all test data are taken from [19]. Three thermal generators and one wind farm are included, and the total load demand P_d is 600 MW. The population n, $f_{\min}$ and $f_{\max}$ are set as 40, 0, and 1, respectively. The loudness A_i and pulse emission rate r_i are replaced by chaotic maps as stated before.

Firstly, no constraint is included in the model. Let the initial values of P_i and W_j are both between 0 and 600 MW randomly. Two random simulation results for active power output are displayed in Fig. 3.

In Fig. 3 (a), the optimal solution is P_1=365.0168 MW, P_2=105.0158 MW, P_3=29.3694 MW and W_1=100.5956 MW with the total cost 5611.8 \$/h. In Fig. 3 (b), the optimal solution is P_1=370.2914 MW, P_2=99.8921 MW, P_3=28.2900 MW and W_1=101.5138 MW with the total cost 5611.7 \$/h. Since no constraint is included, solutions in the iteration process may be negative (see Fig. 3 (a)). The number of steps for convergence in Fig. 3 is 155 and 96, respectively. However, from Fig. 5(a) in [19], the number is about 300000, which is much larger than that in RCBA, but the two methods have almost the same costs (it is 5611.8 \$/h in [19]). The cost convergence curve for Fig. 3 (a) is shown in Fig. 4 (a).

Secondly, the constraints (4) and (5) are included, and two random simulation results are shown in Fig. 5. The first optimal solution is P_1=353.30 MW, P_2=100.00 MW, P_3=50.00 MW and W_1=96.69 MW with the total cost 5614.35 \$/h in Fig. 5 (a), and in Fig. 5 (b), the optimal solution is P_1=352.43 MW, P_2=100.00 MW, P_3=50.00 MW and W_1=97.57 MW with the total cost 5614.40 \$/h. Fig. 5 indicates that the minimum value of TG3 is limited to 50 MW due to the constraints. But in Fig. 3 (a) and Fig. 3 (b), the value of TG3 are both less than 50 MW. Therefore, the final costs in Fig. 5 are a little larger than those in Fig. 3 because of the existence of constraints. The total cost convergence curve for Fig. 5 (a) is shown in Fig. 4 (b).

The comparison results of total costs with constraints are listed in Table VI, in which the data for the 3rd and 4th rows come from P1579 and P1581 in [19], respectively. Table VI indicates that the two random solutions obtained by RCBA

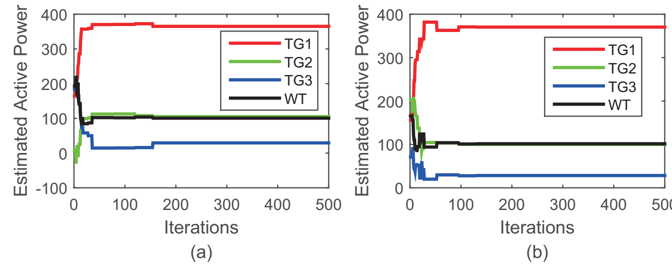

Fig. 3. Two random simulation results for active power output without constraints for case 1.

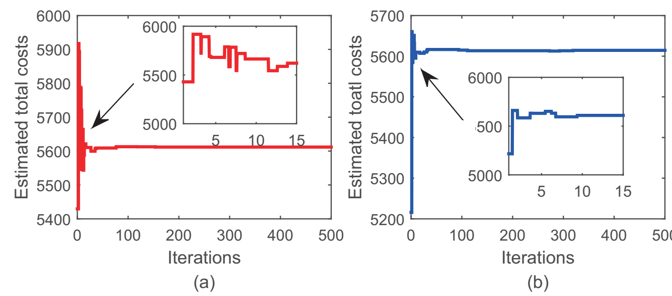

Fig. 4. (a) The cost convergence curve for Fig. 3 (a). (b) The cost convergence curve for Fig. 5 (a).

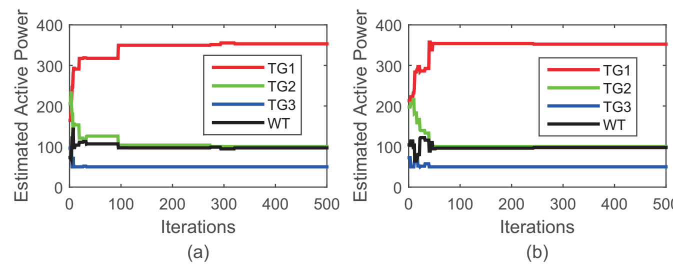

Fig. 5. Two random simulation results for active power output with constraints for case 1.

TABLE VI
COMPARISON OF TOTAL COSTS WITH CONSTRAINTS FOR CASE 1

Items	P_1	P_2	P_3	W_1	cost
RCBA(a)	353.30	100.00	50.00	96.69	**5614.35**
RCBA(b)	352.43	100.00	50.00	97.57	**5614.40**
Algorithm [19]	351.78	100.02	50.02	98.17	5614.45
GA [19]	349.06	103.57	50.03	97.38	5614.7

are both superior to those obtained by the other two methods. Therefore, the effectiveness of the proposed RCBA for EDPs with random wind power is demonstrated.

2) Case 2: *Implementation for EDP with all constraints aforementioned*

Six thermal generators, 26 buses and 46 transmission lines are included in this case, and the total load demand is 1263 MW. In order to compare the performance of RCBA with other algorithms, no wind turbines are included in cases 2 and 3. All the constraints aforementioned in this paper are included in this case, and the test parameters are taken from [8].

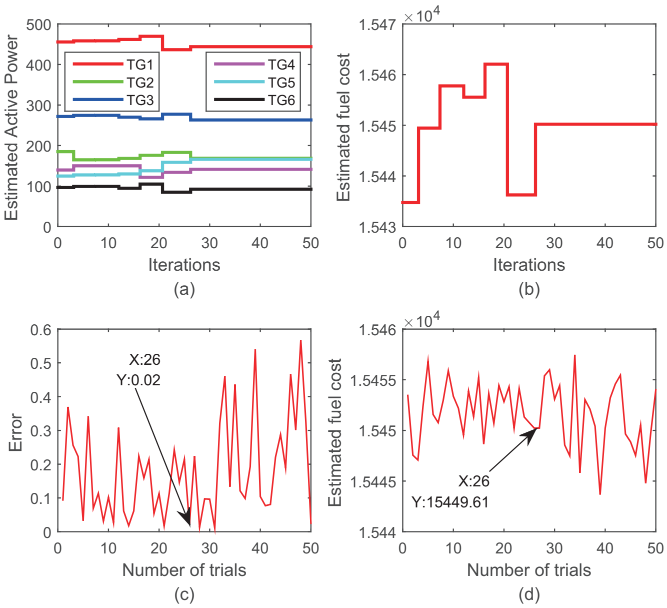

Fig. 6. (a) The active power output simulation results of the 26th trial for case 2 with RCBA. (b) The fuel cost convergence curve of the 26th trial for case 2 with RCBA. (c) The errors for estimated fuel costs with 50 trials for case 2. (d) Estimated fuel costs with 50 trials for case 2.

In this case, the population n is selected as 200, and the number of iterations N_{iter} is set to 50. Total 50 trials are executed and the simulation results are shown in Fig. 6. The convergence curves of the 26th trial for active power output and fuel cost are given in Fig. 6 (a) and Fig. 6 (b), respectively. The errors and estimated fuel costs of the 50 trials are given in Fig. 6 (c) and Fig. 6 (d), respectively. The errors are defined as $e(m) = \left|\sum_{k=1}^{N_g} P_k - P_d - P_{\text{loss}}(m)\right|$, and $m \in [1, 50]$. There are two rules for selecting the optimal solutions in the 50 trials, one is $\sum_{k=1}^{N_g} P_k < C1$, the other is $e(m) < C2$, where C1 and C2 are both constants. According to the rules, the 26th trial is selected as the optimal solution, and the results are shown in Table VII. Table VIII shows the comparison results of several algorithms with RCBA. In Table VII, $\sum P_i$, P_{loss} and *Fuel_cost* denote the sum of P_1 to P_6, transmission line losses, and fuel costs of thermal generators, respectively. In Table VIII, *Ave_cost*, *Max_cost*, *Min_cost*, *CPU_time* and *Steps* are the average, maximum, minimum fuel costs during the iteration, computing time for CPU, and the number of convergence step for the optimal solution of case 2, respectively.

TABLE VII
THE OPTIMAL SOLUTIONS OF 26-BUS SYSTEM FOR CASE 2

Items	RCBA	PSO [8]	GA [8]	CBA [27]
P_1	444.7021	447.4970	474.8066	447.4187
P_2	175.9130	173.3221	178.6363	172.8255
P_3	256.3328	263.4745	262.2089	264.0759
P_4	142.2861	139.0594	134.2826	139.2469
P_5	169.9175	165.4761	151.9039	165.6526
P_6	86.6873	91.27812	74.1812	86.7625
$\sum P_i$	**1275.84**	1276.01	1276.03	1275.982
P_{loss}	**12.9266**	12.9584	13.0217	12.9848
Fuel_cost	**15449.61**	15450	15459	15450.23

CBA: chaotic bat algorithm

TABLE VIII
THE COMPARISON RESULTS FOR CASE 2 (50 TRIALS)

Algorithm	Max_Cost	Min_Cost	Ave_Cost	CPU_time	Steps
RCBA	**15462.23**	**15443.66**	**15452.16**	23.91	**26**
PSO [8]	15492	15450	15454	**14.89**	–
GA [8]	15524	15459	15469	41.58	–
CBA [27]	15518.65	15450.23	15454.76	35.2	>250

In Table VII, the total active power $\sum P_i$, transmission line losses P_{loss} and fuel cost *Fuel_cost* obtained by RCBA are all the smallest among those obtained by the listed algorithms. In Table VIII, the data of RCBA comes from the 26th trial in Fig. 6 (d). The comparison results indicate that RCBA has the smallest values in all comparison items except *CPU_time*. The number of steps for convergence in Fig. 6 (b) is 26, but the corresponding value in [27] is greater than 250. Therefore, RCBA has better performance than PSO, GA and chaotic bat algorithm by the comparison.

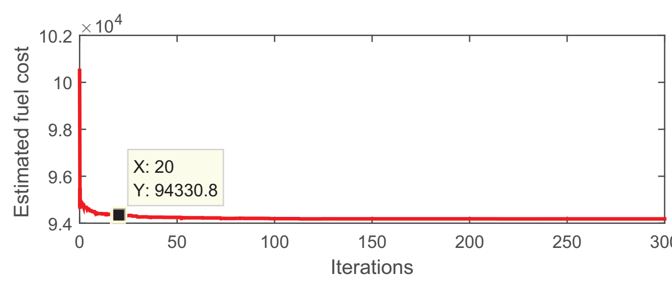

Fig. 7. The fuel cost convergence curve for case 3 with RCBA.

3) Case 3: *Implementation on a system with 38 generators*

The system contains 38 thermal generators. No constraint is included in this case since the purpose here is to evaluate whether RCBA is suitable to high dimensional system or not for power systems. The test data are taken from [36] and the total load demand is 6000 MW.

In this case, the population n, iterations N_{iter} and dimension d are set as 5000, 300, and 38, respectively. We run the simulation for 4 trials every time and the function *parfor* in MATLAB is used to accelerate the simulation speed. The computing time for 4 trials is 45.79 seconds.

Fig. 7 shows the simulation result of fuel cost, in which the convergence value is 94183.99 $/h. The active power output simulation results are not given as there exists 38 curves, and hence it is hardly to see them clearly. Table IX gives the optimal active power output for this case, and Table X gives the comparison results with other algorithms.

TABLE IX
BEST ACTIVE POWER OUTPUT FOR CASE 3

TGs	Output	TGs	Output	TGs	Output
P_1	448.0200	P_{14}	90.0004	P_{27}	38.2371
P_2	430.1260	P_{15}	82.0004	P_{28}	20.0004
P_3	448.1876	P_{16}	120.000	P_{29}	20.0004
P_4	428.7942	P_{17}	161.848	P_{30}	20.0004
P_5	432.8496	P_{18}	65.0004	P_{31}	20.0004
P_6	418.5107	P_{19}	65.0004	P_{32}	20.0004
P_7	389.5183	P_{20}	271.593	P_{33}	25.0004
P_8	423.8822	P_{21}	271.138	P_{34}	18.0004
P_9	114.0004	P_{22}	259.782	P_{35}	8.00042
P_{10}	114.0004	P_{23}	124.400	P_{36}	25.0004
P_{11}	124.1179	P_{24}	10.0004	P_{37}	21.1384
P_{12}	137.0802	P_{25}	119.777	P_{38}	20.0004
P_{13}	110.0004	P_{26}	84.9791	$\sum P_i$	6000.00

DE/BBO: differential evolution with biogeography-based optimization [35];
BBO: biogeography-based optimization [35];
PSO_TVAC: PSO with time-varying acceleration coefficients [37];
NPSO: a new PSO [40]; PSO_Crazy: PSO with craziness operator [41];
SPSO: simple PSO, i.e., the standard PSO

TABLE X
COMPARISON RESULTS OF FUEL COSTS FOR CASE 3

RCBA	DE/BBO [35]	BBO [35]	PSO_TVAC [37]
94183.99	**94172.35**	94176.33	95004.48
NPSO [37]	PSO_Crazy [37]	SPSO [37]	
95164.48	95200.24	95439.84	

The solutions for the other algorithms are not listed due to the space limitation, and interested readers are referred to [35] and [37] for details. It is clear from Table X that the fuel cost values obtained by RCBA, DE/BBO and BBO are comparatively less compared with all PSO-based algorithms and the fuel cost value with RCBA is only a few larger than that with DE/BBO or BBO. The solution with RCBA cannot be improved further more due to the limitation of memory on PC.

Compared with DE/BBO (see Fig. 2 in [35]), our algorithm has obviously good convergence characteristic. In Fig. 7, the fuel cost reaches 94330.8 $/h at the 20th step. But at the same step in [35], the fuel cost is about 96000 $/h, which is much larger than 94330.8 $/h. Therefore, the effectiveness of RCBA for high dimensional systems is demonstrated.

V. CONCLUDING REMARKS

In this paper, a novel hybrid algorithm RCBA has been proposed by integrating chaotic maps and random black hole model into bat algorithm. We have illustrated the effectiveness of the proposed algorithm with five typical benchmark functions, and analyzed why RCBA is successful in avoiding premature convergence problem and accelerating convergence speed. We have also successfully applied RCBA to solve EDP incorporating thermal generators and wind turbines considering random wind power, and demonstrated the effectiveness of using RCBA to deal with high dimensional case for power systems. It should be pointed out that all simulations in this paper do not include valve-point effects, and this problem is left as a future work. The proposed algorithm is also suitable to deal with multiobjective optimization problems, which is another interesting future direction.

REFERENCES

[1] X. P. Li, L. X. Fang, Z. G. Lu, J. F. Zhang, and H. Zhao, "A line flow granular computing approach for economic dispatch with line constraints," *IEEE Trans. Power Syst.*, vol. 32, no. 6, pp. 4832–4842, Nov. 2017.

[2] T. Jayabarathi, T. Raghunathan, B. R. Adarsh, and P. N. Suganthan, "Economic dispatch using hybrid grey wolf optimizer," *Energy*, vol. 111, pp. 630–641, Sep. 2016.

[3] A. J. Wood, B. F. Wollenberg, and G. B. Sheble, *Power Generation, Operation, and Control*, 3rd ed. New York. NY. USA: Wiley, 2012.

[4] K. Y. Lee, Y. M. Park, and J. L. Ortiz, "Fuel-cost minimisation for both real and reactive power dispatches," *Proc. Inst. Elect. Eng., Gen., Tranm. Distrib.*, vol. 131, no. 3, pp. 85–93, 1984.

[5] Y. Guo, L. Tong, W. C. Wu, B. M. Zhang, and H. B. Sun, "Coordinated multi-area economic dispatch via critical region projection," *IEEE Trans. Power Syst.*, vol. 32, no. 5, pp. 3736–3746, Sep. 2017.

[6] D. C. Walters and G. B. Sheble, "Genetic algorithm solution of economic dispatch with valve point loading," *IEEE Trans. Power Syst.*, vol. 8, no. 3, pp. 1325–1332, Aug. 1993.

[7] C. L. Chiang, "Improved genetic algorithm for power economic dispatch of units with valve-point effects and multiple fuels," *IEEE Trans. Power Syst.*, vol. 20, no. 4, pp. 1690–1699, Nov. 2005.

[8] Z. L. Gaing, "Particle swarm optimization to solving the economic dispatch considering the generator constraints," *IEEE Trans. Power Syst.*, vol. 18, no. 3, pp. 1187–1195, Aug. 2003.

[9] Q. D. Qin, S. Cheng, X. H. Chu, X. J. Lei, and Y. H. Shi, "Solving non-convex/non-smooth economic load dispatch problems via an enhanced particle swarm optimization," *Appl. Soft Comput.*, vol. 59, pp. 229–242, Oct. 2017.

[10] L. T. A. Bahrani and J. C. Patra, "Orthogonal PSO algorithm for economic dispatch of thermal generating units under various power constraints in smart power grid," *Appl. Soft Comput.*, vol. 58, pp. 401–426, Sep. 2017.

[11] T. A. A. Victoire and A. E. Jeyakumar, "Hybrid PSO-SQP for economic dispatch with valve-point effect," *Elect. Power Syst. Res.*, vol. 71, no. 1, pp. 51–59, Sep. 2004.

[12] M. Basu, "Artificial bee colony optimization for multi-area economic dispatch," *Int. J. Elect. Power Energy Syst.*, vol. 49, pp. 181–187, Jul. 2013.

[13] B. Jeddi and V. Vahidinasab, "A modified harmony search method for environmental/economic load dispatch of real-world power systems," *Energy Convers. Manage*, vol. 78, pp. 661–675, Feb. 2014.

[14] T. Sen and H. D. Mathur, "A new approach to solve Economic Dispatch problem using a Hybrid ACO-ABC-HS optimization algorithm," *Int. J. Elect. Power Energy Syst.*, vol. 78, pp. 735–744, Jun. 2016.

[15] World Wind Energy Association (WWEA). [Online]. Available: http://www.wwindea.org/wwea-half-year-report-worldwind-wind-capacity-reached-456-gw/.

[16] M. Y. Li, J. Hou, Y. G. Niu, and J. Z. Liu, "Economic dispatch of wind-thermal power system by using aggregated output characteristics of virtual power plants," in *Proc. 12th IEEE Int. Conf. Control Autom.*, Kathmandu, Nepal, 2016, pp. 830–835.

[17] X. Liu, "Economic load dispatch constrained by wind power availability: A wait-and-see approach," *IEEE Trans. Smart Grid*, vol. 1, no. 3, pp. 347–355, Dec. 2010.

[18] L. Yong and S. Tao, "Economic dispatch of power system incorporating wind power plant," in *Proc. Power Eng. Conf.*, 2007, pp. 159–162.

[19] F. H. Guo, C. Y. Wen, J. F. Mao, and Y. D. Song, "Distributed economic dispatch for smart grids with random wind power," *IEEE Trans. Smart Grid*, vol. 7, no. 3, pp. 1572–1583, May 2016.

[20] X. S. Yang, "A new metaheuristic bat-inspired algorithm," in *Nature inspired cooperative strategies for optimization (NICSO 2010) vol. 284*, Springer, Berlin, 2010, pp. 65–74.

[21] S. Mirjalili, S. M. Mirjalili, and X. S. Yang, "Binary bat algorithm," *Neural Comput. Appl.*, vol. 25, no. 3–4, pp. 663–681, Sep. 2014.

[22] A. H. Gandomi and X. S. Yang, "Chaotic bat algorithm," *J. Comput. Sci.*, vol. 5, no. 2, pp. 224–232, Mar. 2014.

[23] S. Yilmaz and E. U. Kucuksille, "A new modification approach on bat algorithm for solving optimization problems," *Appl. Soft Comput.*, vol. 28, pp. 259–275, Mar. 2015.

[24] X. S. Yang and A. Hossein Gandomi, "Bat algorithm: a novel approach for global engineering optimization," *Eng. Comput.*, vol. 29, no. 5, pp. 464–483, 2012.

[25] Black holes. [Online]. Available: http://hyperphysics.phy-astr.gsu.edu/hbase/Astro/blkhol.html.

[26] Black hole. [Online]. Available: https://en.wikipedia.org/wiki/Black_hole.

[27] B. R. Adarsh, T. Raghunathan, T. Jayabarathi, and X. S. Yang, "Economic dispatch using chaotic bat algorithm," *Energy*, vol. 96, pp. 666–675, Feb. 2016.

[28] J. Q. Zhang, K. Liu, Y. Tan, and X. G. He, "Random black hole particle swarm optimization and its application," in *Proc. IEEE Int. Conf. Neural Netw. Signal Process*, Nanjing, China, 2008, pp. 359–365.

[29] J. Hetzer, C. Y. David, and K. Bhattarai, "An economic dispatch model incorporating wind power," *IEEE Trans. Energy Convers.*, vol. 23, no. 2, pp. 603–611, Jun. 2008.

[30] X. Liu and W. Xu, "Minimum emission dispatch constrained by stochastic wind power availability and cost," *IEEE Trans. Power Syst.*, vol. 25, no. 3, pp. 1705–1713, Aug. 2010.

[31] B. Akay and D. Karaboga, "A modified Artificial Bee Colony algorithm for real–parameter optimization," *Inf. Sci.*, vol. 192, pp. 120–142, Jun. 2012.

[32] S. Strasser, J. Sheppard, N. Fortier, and R. Goodman, "Factored evolutionary algorithms," *IEEE Trans. Evol. Comput.*, vol. 21, no. 2, pp. 281–293, Apr. 2017.

[33] X. J. Du, J. L. Wang, V. Jegatheesan, and G. H. Shi, "Parameter estimation of activated sludge process based on an improved cuckoo search algorithm," *Bioresour. Technol.*, vol. 249, pp. 447–456, Feb. 2018.

[34] S. Mirjalili, S. M. Mirjalili, and A. Lewisi, "Grey wolf optimizer," *Adv. Eng. Softw.*, vol. 69, pp. 46–61, Mar. 2014.

[35] A. Bhattacharya and P. K. Chattopadhyay, "Hybrid differential evolution with biogeography based optimization for solution of economic load dispatch," *IEEE Trans. Power Syst.*, vol. 25, no. 4, pp. 1995–1964, Nov. 2010.

[36] M. Sydulu, "A very fast and effective non-iterative 'λ-logic based' algorithm for economic dispatch of thermal units," in *Proc. IEEE Region 10 Conf. TENCON*, 1999, pp. 1434–1437.

[37] K. T. Chaturvedi, M. Pandit, and L. Srivastava, "Particle swarm optimization with time varying acceleration coefficients for non-convex economic power dispatch," *Int. J. Elect. Power Energy Syst.*, vol. 31, no. 6, pp. 249–257, Jul. 2009.

[38] S. Suresh and S. Lal, "Multilevel thresholding based on chaotic darwinian particle swarm optimization for segmentation of satellite images," *Appl. Soft Comput.*, vol. 55, pp. 503–522, Jun. 2017.

[39] P. Li, D. Xu, Z. Y. Zhou, W. J. Lee, and B. Zhao, "Stochastic optimal operation of microgrid based on chaotic binary particle swarm optimization," *IEEE Trans. Smart Grid.*, vol. 7, no. 1, pp. 66–73, Jan. 2016.

[40] A. Immanuel Selvakumar and K. Thanushkodi, "A new particle swarm optimization solution to nonconvex economic dispatch problems," *IEEE Trans. Power Syst.*, vol. 22, no. 1, pp. 42–51, Feb. 2007.

[41] T. Aruldoss Albert Victoire and A. Ebenezer Jeyakumar, "Reserve constrained dynamic dispatch of units with valve-point effects," *IEEE Trans. Power Syst.*, vol. 20, no. 3, pp. 1273–1282, Aug. 2005.

Huijun Liang received the B.Eng. degree in industry automation from Wuhan University of Hydraulic and Electric Engineering, Wuhan, China, in 2000, and the M.Eng. degree in control theory and control engineering from Wuhan University, Wuhan, China, in 2004. He is currently pursuing the Ph.D. degree in Shandong University, Jinan, China.

His current research interests include intelligent computing, optimal control in power systems.

Yungang Liu received the Ph.D. degree in control theory and control engineering from Shanghai Jiao Tong University, Shanghai, China, in 2000.

He is now a Changjiang Scholar Chair Professor with the School of Control Science and Engineering, Shandong University, Jinan, China. His current research interests include stochastic control, nonlinear control design and system analysis, adaptive control and applications in power systems, and big data.

Dr. Liu was a recipient of the Guan Zhaozhi Award in the Chinese Control Conference in 2004, the National Outstanding Youth Science Foundation of China in 2013, and the Second Prize of the National Natural Science Award of China in 2015. He currently serves as an Associate Editor for seven famous scientific journals.

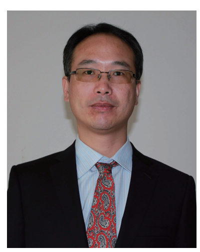

Yanjun Shen received the Ph.D. degree in the Department of Control and Engineering at Huazhong University of Science and Technology in 2004. Currently, he is a professor in the College of Electrical Engineering and New Energy, China Three Gorges University.

His research interests include robust control, nonlinear systems, neural networks.

Fengzhong Li received the Ph.D. degree in Control Theory and Control Engineering from Shandong University in June 2016. He is a recipient of National Scholarship for Ph.D. students of China in 2015. Currently, he works as a postdoctoral scholar in the same university.

His current research interests include stochastic control, nonlinear control, adaptive control and time-varying control.

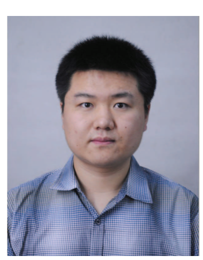

Yongchao Man received the Ph.D. degree in Control Theory and Control Engineering from Shandong University in December 2015. He is a recipient of National Scholarship for Ph.D. students of China in 2012. Currently, he works as a postdoctoral scholar in the same university.

His current research interests include nonlinear control, adaptive control and time-varying control and big-data analysis.